Quantum Transport Evidence for the Three-Dimensional Dirac Semimetal Phase in Cd_3As_2

L. P. He, X. C. Hong, J. K. Dong, J. Pan, Z. Zhang, J. Zhang, and S. Y. Li*
Department of Physics, and Laboratory of Advanced Materials, State Key Laboratory of Surface Physics, Fudan University, Shanghai 200433, People's Republic of China
(Received 21 August 2014; published 9 December 2014)

We report the quantum transport properties of Cd_3As_2 single crystals in a magnetic field. A large linear quantum magnetoresistance is observed near room temperature. With decreasing temperature, the Shubnikov—de Haas oscillations appear in both the longitudinal resistance R_{xx} and the transverse Hall resistance R_{xy}. From the strong oscillatory component ΔR_{xx}, a linear dependence of the Landau index n on $1/B$ is obtained, and it gives an n-axis intercept between $1/2$ and $5/8$. This clearly reveals a nontrivial π Berry's phase, which is a distinguished feature of Dirac fermions. Our quantum transport results provide bulk evidence for the existence of a three-dimensional Dirac semimetal phase in Cd_3As_2.

DOI: 10.1103/PhysRevLett.113.246402 PACS numbers: 71.55.Ak, 71.70.Di, 72.15.Gd

Dirac materials whose excitations obey a relativistic Dirac-like equation have been widely studied in recent years, represented by graphene and topological insulators [1–3]. The Dirac fermions in graphene and the surfaces of topological insulators are two dimensional (2D). In bulk $Bi_{1-x}Sb_x$, a three-dimensional (3D) Dirac point can be realized by finely tuning x, when a topological phase transition occurs [4–7]. However, this 3D Dirac point coexists with additional Fermi surfaces [5]. More recently, a 3D Dirac semimetal has been theoretically predicted, with examples of BiO_2, A_3Bi (A = Na, K, Rb), Cd_3As_2, and some distorted spinels [8–11], in which the Fermi surface only consists of 3D Dirac points with linear energy dispersion in any momentum direction. The 3D Dirac point, where two Weyl points overlap in momentum space, is protected by crystal symmetry [8–11]. By symmetry breaking, this 3D Dirac semimetal can be driven to a topological insulator or Weyl semimetal [10]. The quantum spin Hall effect may be observed in its quantum-well structure and topological superconductivity may be achieved by carrier doping [10]. Since it is a 3D analogue to graphene, the 3D Dirac semimetal could be important for future device applications.

Following these predictions, angle-resolved photoemission spectroscopy (ARPES) experiments were carried out on Na_3Bi and Cd_3As_2 single crystals to probe the novel electronic structure [12–16]. Amazingly, two bulk 3D Dirac points were observed in both compounds, which locate on the opposite sides of the Brillouin zone center point Γ along k_z [12–16]. Recent scanning tunneling microscopy (STM) measurements on a Cd_3As_2 single crystal also support the existence of 3D Dirac points [17].

The bulk quantum transport measurement is another important tool to detect Dirac fermions. Because of their linear energy dispersion, the massless Dirac fermions should manifest a characteristic linear quantum magnetoresistance (MR) at the quantum limit, where all of the carriers occupy the lowest Landau level [18]. This has been previously examined for β-Ag_2Te [19,20], multilayer epitaxial graphene [21], and topological insulators [22–25]. Such a linear quantum MR was also predicted in Cd_3As_2, even up to room temperature [10]. Another distinguished feature of Dirac fermions is the nontrivial π Berry's phase, which results from their cyclotron motion [26–29]. It is a geometrical phase factor, acquired when an electron circles a Dirac point. This Berry's phase can be experimentally accessed by analyzing the Shubnikov—de Haas (SdH) oscillations, which has been widely employed in studies of graphene [28,29], $SrMnBi_2$ [30], topological insulators [22,24,31,32], and the Rashba semiconductor BiTeI [33].

In this Letter, we present the longitudinal resistance and transverse Hall resistance measurements on Cd_3As_2 single crystals in a magnetic field. A large linear MR is observed near room temperature. By analyzing the SdH oscillations of longitudinal resistance at low temperature, a nontrivial π Berry's phase is revealed. This is bulk evidence for the existence of a 3D Dirac semimetal phase in Cd_3As_2, complementary to previous ARPES and STM experiments.

The Cd_3As_2 single crystals were grown from Cd flux with the starting composition Cd : As = 8 : 3, as described in Ref. [34]. The Cd and As powders were put in an alumina crucible after sufficient grinding. The alumina crucible was placed in an iron crucible, which was then sealed in argon atmosphere. The iron crucible was heated to 825 °C and kept for 24 hours, then slowly cooled down to 425 °C at 6 °C/hour. After the alumina crucible was taken out, the excess Cd flux was removed by centrifuging in a quartz tube at 425 °C. The largest natural surface of the obtained Cd_3As_2 single crystals was determined to be the (112) plane by x-ray diffraction, with typical dimension of 2.0×2.0 mm^2. The quality of the Cd_3As_2 single crystals was further checked by the x-ray rocking curve, shown in

the inset of Fig. 1(a). The full width at half maximum (FWHM) is only 0.08°, indicating the high quality of the single crystals. The sample was cut and polished to a bar shape, with 1.70×0.78 mm^2 in the (112) plane and a 0.20 mm thickness. A standard six-probe method was used for both the longitudinal resistivity and transverse Hall resistance measurements. A magnetic field was applied perpendicular to the (112) plane up to 14.5 T.

Figure 1(a) shows the temperature dependence of the longitudinal resistivity ρ_{xx} at zero magnetic field for a Cd_3As_2 single crystal. Below 10 K the curve is very flat, extrapolating to a residual resistivity $\rho_{xx0} \approx 28.2$ $\mu\Omega$ cm. Figure 1(b) presents the Hall resistance R_{xy} as a function of magnetic field at various temperatures. The negative slope of R_{xy} means that the dominant charge carriers in Cd_3As_2 are electrons, and the carrier concentration $n_e \approx 5.3 \times 10^{18}$ cm^{-3} is estimated from the low-field slope. We evaluate the carrier mobility at 1.5 K as $\mu(1.5\ \mathrm{K}) = 1/n_e \rho_{xx}(1.5\ \mathrm{K}) e \approx 4.1 \times 10^4$ cm^2/Vs, where $\rho_{xx}(1.5\ \mathrm{K}) = 28.2$ $\mu\Omega$ cm and $e = 1.6 \times 10^{-19}$ C. The low concentration and high mobility of charge carriers in Cd_3As_2 are well known from early transport studies [35,36] and recent ARPES experiments [14–16].

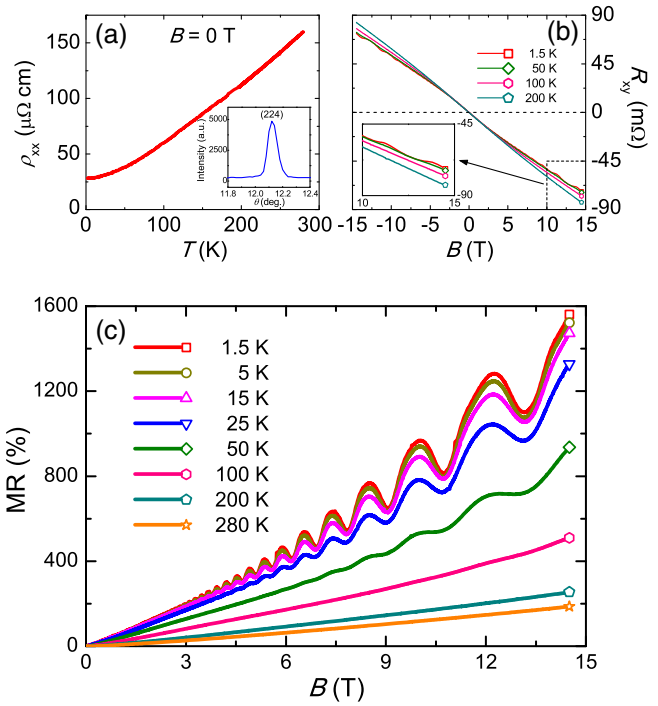

FIG. 1 (color online). (a) The longitudinal resistivity of a Cd_3As_2 single crystal in zero magnetic field, with current in the (112) plane. A typical x-ray rocking curve of the (224) Bragg peak is shown in the inset. (b) The Hall resistance R_{xy} at 200, 100, 50, and 1.5 K. There are clear oscillations of R_{xy} at 1.5 K, as seen in the inset. (c) The Shubinikov—de Haas oscillations of longitudinal magnetoresistance (MR) at various temperatures, with the field perpendicular to the (112) plane. At 280 K, the MR is roughly linear without saturation, as high as 200% at $B = 14.5$ T. At 1.5 K, the oscillations appear at a field as low as 2 T, reflecting the high mobility of charge carriers in Cd_3As_2.

In Fig. 1(b), there are clear oscillations of R_{xy} at 1.5 K. R_{xx} shows even more pronounced SdH oscillations, as can be seen from the longitudinal MR in Fig. 1(c). The MR is defined by $\mathrm{MR} = [R_{xx}(B) - R_{xx}(0\ \mathrm{T})]/R_{xx}(0\ \mathrm{T}) \times 100\%$. At 280 K, the MR shows no sign of saturation in high field, as high as 200% at 14.5 T. Previously, the MR of Cd_3As_2 single crystals was measured up to 3.1 T at 77 and 300 K by Radautsan *et al.* [37]. They observed MR $\approx 16\%$ at 3.1 T and 300 K, which is lower than the value MR $\approx 27\%$ at 3.1 T and 280 K in Fig. 1(c). Above 3 T, the MR of our Cd_3As_2 single crystal is quite linear, which is consistent with the theoretical prediction [10]. However, the quantum limit required in Ref. [10] is actually not reached in our sample, since there is clearly more than one Landau level occupied in our field range, as will be seen in Fig. 2(a). Similar situations exist in multilayer epitaxial graphene [21] and the topological insulators Bi_2Se_3 and Bi_2Te_3 [22,24,25]. To understand the physical origin of the linear MR without reaching the quantum limit, further theoretical studies are highly desired. Nevertheless, this large room-temperature linear MR is quite unusual. If its magnitude can be further enhanced, Cd_3As_2 may be useful for practical applications in magnetic random access memory and magnetic sensors.

With decreasing temperature, the MR increases dramatically. At 1.5 K, the MR oscillations can be tracked down to a field as low as $B \approx 2$ T, reflecting the high mobility of the charge carriers. In Fig. 2(a), we show the oscillatory component of ΔR_{xx} versus $1/B$ at various temperatures after subtracting a smooth background. They are periodic in $1/B$, as expected from the successive emptying of the Landau levels when the magnetic field is increased. A single oscillation frequency $F = 58.3$ T is identified from fast Fourier transform spectra, which corresponds to $\Delta(1/B) = 0.0171$ T^{-1}. According to the Onsager relation $F = (\Phi_0/2\pi^2)A_F$, the cross-sectional area of the Fermi surface normal to the field is $A_F = 5.6 \times 10^{-3}$ Å^{-2}. By assuming a circular cross section, a very small Fermi momentum $k_F \approx 0.042$ Å^{-1} is estimated. This result is in good agreement with a recent ARPES experiment, which shows that the Fermi surface of Cd_3As_2 consists of two tiny ellipsoids or almost spheres with $k_F \approx 0.04$ Å^{-1} [16]. Note that these two ellipsoids are equivalent; therefore, there should be only one oscillation frequency F, as we observed. From another ARPES study on a Cd_3As_2 single crystal with a comparable carrier concentration, the distance between the Dirac point and the high-symmetry Γ point is about 0.15 Å^{-1} [15]. Such a value is much larger than our k_F, which means that our sample is not close to the Lifshitz transition (i.e., the Fermi level reaches the valence band top).

The SdH oscillation amplitude can be described by the Lifshitz-Kosevich formula [33,38]

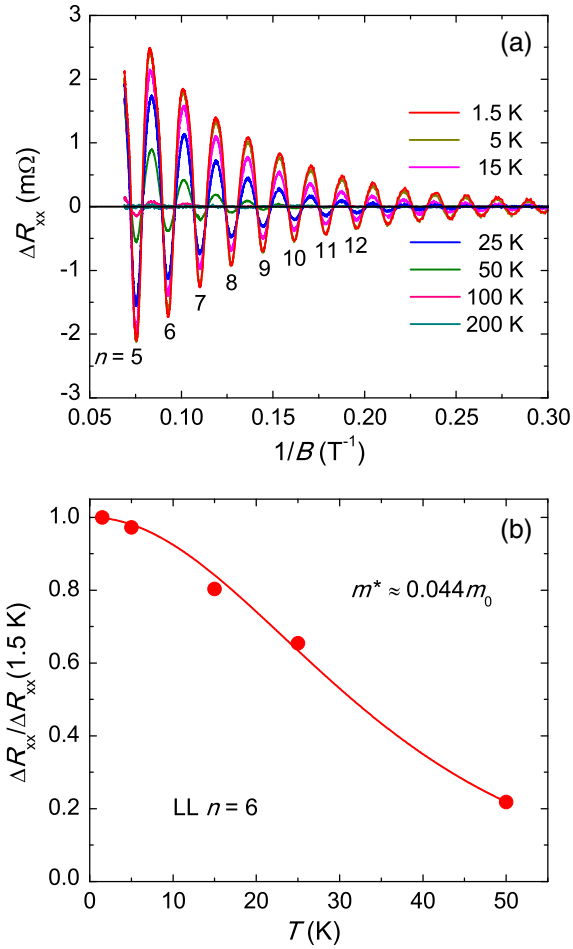

FIG. 2 (color online). (a) The oscillatory component ΔR_{xx}, extracted from R_{xx} by subtracting a smooth background, as a function of $1/B$ at various temperatures. A single oscillation frequency $F = 58.3$ T is identified from fast Fourier transform spectra. (b) The temperature dependence of the relative amplitude of ΔR_{xx} for the sixth Landau level. The solid line is a fit to the Lifshitz-Kosevich formula, from which we get the cyclotron effective mass $m^* \approx 0.044 m_0$ and Fermi velocity $v_F \approx 1.1 \times 10^6$ m/s.

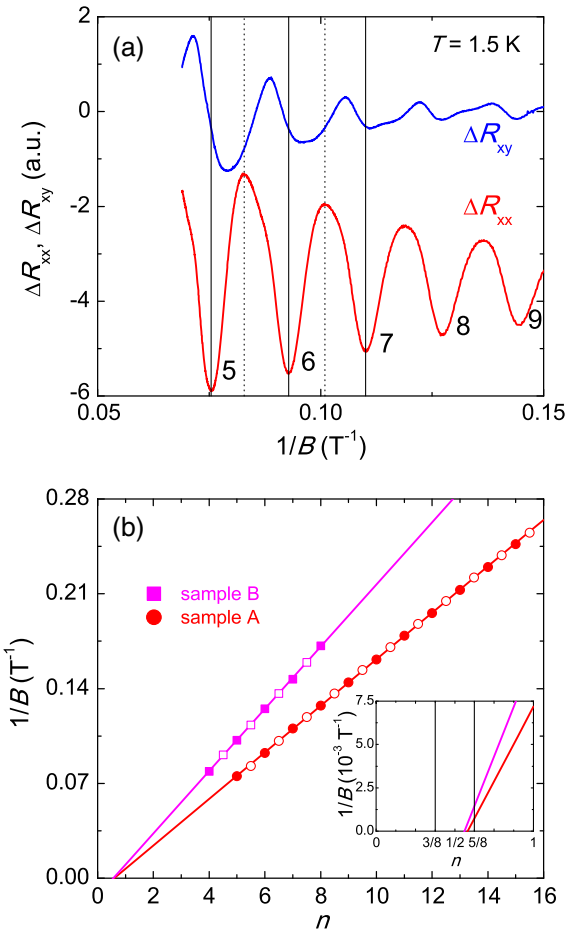

FIG. 3 (color online). (a) The high-field oscillatory components ΔR_{xx} and ΔR_{xy} at 1.5 K. The ΔR_{xy} oscillations are phase shifted approximately by 90° with respect to the ΔR_{xx} oscillations for the low Landau levels. No Landau level splitting is observed in our field range. (b) Landau index n plotted against $1/B$. The closed circles denote the integer index (ΔR_{xx} valley), and the open circles indicate the half integer index (ΔR_{xx} peak). The index plot can be linearly fitted, giving the intercept 0.58 ± 0.01. The measurements of another single crystal labeled as sample B (see the Supplemental Material [39]) give a similar intercept 0.56 ± 0.03. From the inset, both intercepts of ΔR_{xx} lie between β and $\beta + 1/8 (\beta = 1/2)$, which is strong evidence for a nontrivial π Berry's phase of 3D Dirac fermions in Cd_3As_2.

$$\Delta\rho_{xx} \propto \frac{2\pi^2 k_B T/\hbar\omega_c}{\sinh(2\pi^2 k_B T/\hbar\omega_c)} e^{-2\pi^2 k_B T_D/\hbar\omega_c} \cos 2\pi \times \left(\frac{F}{B} + \frac{1}{2} + \beta\right), \quad (1)$$

where ω_c is the cyclotron frequency and T_D is the Dingle temperature. $2\pi\beta$ is the Berry's phase, which will be discussed later. Figure 2(b) plots the temperature dependence of the normalized oscillation amplitude at $1/B = 0.0928$ T^{-1}, which corresponds to the sixth Landau level. The energy gap $\hbar\omega_c$ can be obtained from the thermal damping factor $R_T = (2\pi^2 k_B T/\hbar\omega_c / \sinh(2\pi^2 k_B T/\hbar\omega_c))$. The solid line in Fig. 2(b) is the best fit to the data, which yields $\hbar\omega_c(n = 6) \approx 24.6$ meV. For a Dirac system, the cyclotron frequency ω_c follows a square root dependence on the magnetic field. By employing $E_n = v_F\sqrt{2e\hbar nB}$ and $v_F = \hbar k_F/m^*$, a rather small cyclotron effective mass $m^* \approx 0.044 m_0$ and a very large Fermi velocity $v_F \approx 1.1 \times 10^6$ m/s are obtained. This value of v_F is very close to the ARPES result $\sim 1.5 \times 10^6$ m/s in Ref. [15]. Such a large Fermi velocity may explain the unusual high mobility in Cd_3As_2.

Figure 3(a) plots together the oscillatory components ΔR_{xx} and ΔR_{xy} at the lowest temperature $T = 1.5$ K. There are two clear features. First, the ΔR_{xy} oscillations are phase shifted approximately by 90° with respect to the ΔR_{xx} oscillations for the low Landau levels, as expected [24]. Secondly, no Landau level splitting is observed in our

field range ($n \geq 5$). This is consistent with a recent STM experiment, in which the Landau level splitting was only observed for $n \leq 4$ [17]. Figure 3(b) is the Landau index plot, n versus $1/B$, for ΔR_{xx}. We assign integer indices to the ΔR_{xx} valley positions in $1/B$ and half integer indices to the ΔR_{xx} peak positions. According to the Lifshitz-Onsager quantization rule $A_F(\hbar/eB) = 2\pi(n + 1/2 + \beta + \delta)$, the Landau index n is linearly dependent on $1/B$. $2\pi\beta$ is the Berry's phase, and $2\pi\delta$ is an additional phase shift resulting from the curvature of the Fermi surface in the third direction [33]. δ changes from 0 for a quasi-2D cylindrical Fermi surface to $\pm 1/8$ for a corrugated 3D Fermi surface [33]. Our data points in Fig. 3(b) fall into a very straight line, and the linear extrapolation gives an intercept 0.58 ± 0.01. We also measured another Cd_3As_2 single crystal with less pronounced SdH oscillations (see the Supplemental Material for details [39]), and the linear extrapolation gives nearly the same intercept 0.56 ± 0.03, shown in Fig. 3(b).

In the trivial parabolic dispersion case such as that involving conventional metals, the Berry's phase $2\pi\beta$ should be zero. For Dirac systems with linear dispersion, there should be a nontrivial π Berry's phase ($\beta = 1/2$). This π Berry's phase has been clearly observed in 2D graphene [28,29], and in bulk $SrMnBi_2$ in which highly anisotropic Dirac fermions reside in the 2D Bi square net [30]. For topological insulators Bi_2Se_3 and Bi_2Te_3 with gapless 2D Dirac fermions at their surfaces, the search for the π Berry's phase was complicated by large Zeeman energy effects and bulk conduction [22,24,31,32]. The bulk Rashba semiconductor BiTeI also possesses a Dirac point and provides an alternative path to realizing the nontrivial π Berry's phase, which was indeed experimentally detected [33]. The intercept 0.58 ± 0.01 obtained in Fig. 3(b) clearly reveals the π Berry's phase, and thus provides strong evidence for the existence of Dirac fermions in Cd_3As_2. The slight deviation from $\beta = 1/2$ indicates an additional phase shift $\delta \approx 0.08$, which may result from the 3D nature of the system [33]. Complementary to previous ARPES and STM experiments [14–17], our bulk transport measurements confirm the 3D Dirac semimetal phase in Cd_3As_2.

In summary, we have performed bulk transport measurements on single crystals of the proposed 3D Dirac semimetal Cd_3As_2. A large linear quantum magnetoresistance is observed near room temperature. By analyzing the Shubnikov—de Haas oscillations of longitudinal resistance at low temperature, a nontrivial π Berry's phase with a small phase shift is obtained, which provides bulk quantum transport evidence for the existence of a 3D Dirac semimetal phase in Cd_3As_2. With its unique electronic structure, unusual high mobility, and large room-temperature linear magnetoresistance, the 3D Dirac semimetal Cd_3As_2 may open new avenues for future device applications.

We thank D. L. Feng, J. Jiang, X. F. Jin, Y. Y. Wang, Z. Wang, H. M. Weng, Z. J. Xiang, H. Yao, and Y. B. Zhang for fruitful discussions. This work is supported by the Ministry of Science and Technology of China (National Basic Research Program No. 2012CB821402), the Natural Science Foundation of China, and the Program for Professor of Special Appointment (Eastern Scholar) at Shanghai Institutions of Higher Learning.

*shiyan_li@fudan.edu.cn

[1] A. H. Castro Neto, F. Guinea, N. M. R. Peres, K. S. Novoselov, and A. K. Geim, Rev. Mod. Phys. **81**, 109 (2009).
[2] M. Z. Hasan and C. L. Kane, Rev. Mod. Phys. **82**, 3045 (2010).
[3] X.-L. Qi and S.-C. Zhang, Rev. Mod. Phys. **83**, 1057 (2011).
[4] L. S. Lerner, K. F. Cuff, and L. R. Williams, Rev. Mod. Phys. **40**, 770 (1968).
[5] D. Hsieh, D. Qian, L. Wray, Y. Xia, Y. S. Hor, R. J. Cava, and M. Z. Hasan, Nature (London) **452**, 970 (2008).
[6] S. Tang and M. S. Dresselhaus, Nano Lett. **12**, 2021 (2012).
[7] S. Tang and M. S. Dresselhaus, Nanoscale **4**, 7786 (2012).
[8] S. M. Young, S. Zaheer, J. C. Y. Teo, C. L. Kane, E. J. Mele, and A. M. Rappe, Phys. Rev. Lett. **108**, 140405 (2012).
[9] Z. Wang, Y. Sun, Xing-Qiu Chen, C. Franchini, G. Xu, H. Weng, Xi Dai, and Z. Fang, Phys. Rev. B **85**, 195320 (2012).
[10] Z. Wang, H. Weng, Q. Wu, X. Dai, and Z. Fang, Phys. Rev. B **88**, 125427 (2013).
[11] J. Steinberg, S. M. Young, S. Zaheer, C. L. Kane, E. J. Mele, and A. M. Rappe, Phys. Rev. Lett. **112**, 036403 (2014).
[12] Z. K. Liu, B. Zhou, Y. Zhang, Z. J. Wang, H. M. Weng, D. Prabhakaran, S.- K. Mo, Z. X. Shen, Z. Fang, X. Dai, Z. Hussain, and Y. L. Chen, Science **343**, 864 (2014).
[13] S.-Y. Xu *et al.*, arXiv:1312.7624.
[14] Z. K. Liu *et al.*, Nat. Mater. **13**, 677 (2014).
[15] M. Neupane *et al.*, Nat. Commun. **5**, 3786 (2014).
[16] S. Borisenko, Q. Gibson, D. Evtushinsky, V. Zabolotnyy, B. Büchner, and R. J. Cava, Phys. Rev. Lett. **113**, 027603 (2014).
[17] S. Jeon, B. B. Zhou, A. Gyenis, B. E. Feldman, I. Kimchi, A. C. Potter, Q. D. Gibson, R. J. Cava, A. Vishwanath, and A. Yazdani, Nat. Mater. **13**, 851 (2014).
[18] A. A. Abrikosov, Phys. Rev. B **58**, 2788 (1998).
[19] R. Xu, A. Husmann, T. F. Rosenbaum, M.-L. Saboungi, J. E. Enderby, and P. B. Littlewood, Nature (London) **390**, 57 (1997).
[20] W. Zhang, R. Yu, W. Feng, Y. Yao, H. Weng, Xi Dai, and Z. Fang, Phys. Rev. Lett. **106**, 156808 (2011).
[21] A. L. Frideman *et al.*, Nano Lett. **10**, 3962 (2010).
[22] H. Tang, D. Liang, R. L. Qiu, and X. P. Gao, ACS Nano **5**, 7510 (2011).
[23] H. He, B. Li, Hongchao Liu, Xin Guo, Z. Wang, M. Xie, and J. Wang, Appl. Phys. Lett. **100**, 032105 (2012).
[24] See D. X. Qu, Y. S. Hor, J. Xiong, R. J. Cava, and N. P. Ong, Science **329**, 821 (2010), and its supporting online material.
[25] X. Wang, Y. Du, S. Dou, and C. Zhang, Phys. Rev. Lett. **108**, 266806 (2012).
[26] G. P. Mikitik and Y. V. Sharlai, Phys. Rev. Lett. **82**, 2147 (1999).
[27] G. P. Mikitik and Y. V. Sharlai, Phys. Rev. Lett. **93**, 106403 (2004).

[28] K. S. Novoselov, A. K. Geim, S. V. Morozov, D. Jiang, M. I. Katsnelson, I. V. Grigorieva, S. V. Dubonos, and A. A. Firsov, Nature (London) **438**, 197 (2005).
[29] Y. B. Zhang, Y. W. Tan, H. L. Stormer, and P. Kim, Nature (London) **438**, 201 (2005).
[30] J. Park *et al.*, Phys. Rev. Lett. **107**, 126402 (2011).
[31] J. G. Analytis, R. D. McDonald, S. C. Riggs, Jiun-Haw Chu, G. S. Boebinger, and I. R. Fisher, Nat. Phys. **6**, 960 (2010).
[32] B. Sacepe, J. B. Oostinga, J. Li, A. Ubaldini, N. J. G. Couto, E. Giannini, A. F. Morpurgo, Nat. Commun. **2**, 575 (2011).
[33] H. Murakawa, M. S. Bahramy, M. Tokunaga, Y. Kohama, C. Bell, Y. Kaneko, N. Nagaosa, H. Y. Hwang, and Y. Tokura, Science **342**, 1490 (2013).
[34] M. N. Ali, Q. Gibson, S. Jeon, B. B. Zhou, A. Yazdani, and R. J. Cava, Inorg. Chem. **53**, 4062 (2014).
[35] J.-P. Jay-Gerin, M. J. Aubin, and L. G. Caron, Solid State Commun. **21**, 771 (1977).
[36] L. Zdanowicz, J. C. Portal, and W. Zdanowicz, Lect. Notes Phys. **177**, 386 (1983).
[37] S. I. Radautsan, E. K. Arushanov, and G. P. Chuiko, Phys. Status Solidi A **20**, 221 (1973).
[38] D. Shoenberg, *Magnetic Oscillations in Metals* (Cambridge University Press, Cambridge, England, 1984).
[39] See Supplemental Material at http://link.aps.org/supplemental/10.1103/PhysRevLett.113.246402 for the raw data of sample *B*.